Chapter 2. The Interstellar Medium

Notes:

- *Most of the material presented in this chapter is taken from Stahler and Palla (2004), Chap. 2.*

2.1 The Phases of the Interstellar Medium

We study the different phases, i.e., atomic, ionized, and molecular, under which hydrogen exists in the interstellar medium. Actually molecular hydrogen is not strictly speaking a phase, but we still include it, as it is the main component of molecular clouds.

2.1.1 **Atomic Hydrogen - HI**

We know from the solution of Schrödinger's equation for the hydrogen atom that its different energy levels are given by

$$\begin{aligned} E &= -\frac{\mu_{\rm ep} e^4}{2\hbar^2 n^2} \\ &= -\frac{13.6}{n^2}\ \text{eV}, \end{aligned} \tag{2.1}$$

where $n = 1,2,3,\ldots$ is the **principal quantum number** and $\mu_{\rm ep}$ is the reduced mass. Although such analysis shows that transitions to the lowest levels ($n \to 1$ is the **Lyman series** and $n \to 2$ the **Balmer series**) yield photons at ultraviolet and visible wavelengths (e.g., $n = 2 \to 1$ and $n = 3 \to 2$ are for Lyα at 1216 Å and Hα at 6563 Å photons, respectively) a more complete analysis reveals that it is possible to detect atomic hydrogen at much longer wavelengths, even at very low temperature (if the gas were at high temperature such that high energy levels where occupied, then transitions between such levels would bring about photons of much longer wavelengths).

If we neglect the presence of the electron and proton spins, then total angular momentum $\mathbf{F}$ of the atom is given solely by the orbital angular momentum $\mathbf{L}$ of the electron. The aforementioned solution of Schrödinger's equation shows that the angular momentum is quantized such that the eigenvalues of its square are given by

$$\left\langle |\mathbf{L}|^2 \right\rangle = L(L+1)\hbar^2, \quad \text{with } L = 0,1,2,\ldots,n-1, \tag{2.2}$$

and those of its component along a given axis, say, the z-axis , by

$$\left\langle L_z \right\rangle = m\hbar, \quad \text{with } |m| = 0,1,2,\ldots,L. \tag{2.3}$$

There are therefore n^2 levels of similar energy for every level n. Since photons have a finite energy and an angular momentum (or rather a spin) of value $\hbar$, any **radiative transition** between two energy levels must obey the following **selection rules**

$$\begin{aligned} \hbar\omega &= 13.6\left(\frac{1}{n_{\mathrm{l}}^2}-\frac{1}{n_{\mathrm{u}}^2}\right)\ \mathrm{eV} \\ \Delta L &= \pm 1 \end{aligned} \tag{2.4}$$

because of energy and angular momentum conservation considerations. In equations (2.4) ω is the photon angular frequency, and n_{l} and n_{u} are the lower and upper energy levels that define the transition in question, respectively. Any potential transition that does not obey these rules is said to be **forbidden**.

When the spins are properly taken into account, however, the total angular momentum $\mathbf{F}$ is given by

$$\begin{aligned} \mathbf{F} &= \mathbf{L}+\mathbf{S}+\mathbf{I} \\ &= \mathbf{J}+\mathbf{I}, \end{aligned} \tag{2.5}$$

where $\mathbf{S}$ and $\mathbf{I}$ are the electron and nuclear spins, respectively. When two angular momenta such as $\mathbf{L}$ and $\mathbf{S}$, for example, are coupled together then the square of the resulting angular momentum $\mathbf{J}$ has eigenvalues $J(J+1)\hbar^2$ with

$$|L-S| \le J \le |L+S|. \tag{2.6}$$

Similarly, the total angular momentum in equation (2.5) is characterized by the possible values

$$|J-I| \le F \le |J+I|. \tag{2.7}$$

Moreover, these angular momenta obey rules similar of equations (2.2) and (2.3). For example, for the total angular momentum we have

$$\begin{aligned} \left\langle |\mathbf{F}|^2 \right\rangle &= F(F+1)\hbar^2 \\ \left\langle F_z \right\rangle &= m_F \hbar \end{aligned} \tag{2.8}$$

with the possibility for the quantum numbers F and m_F to be half-integers. Under this more precise model for the hydrogen atom, the second selection rule for radiative transitions of equations (2.4) becomes

$$\Delta F = \pm 1. \tag{2.9}$$

That is, the restriction on ΔL is removed. Moreover, because the electronic and nuclear spins are accompanied by (or stand for the presence of) a magnetic moment there will be an interaction between them that will differentiate the energy levels for states of differing quantum numbers F (i.e., the energy degeneracy is lifted). That is, the first selection rule

of equations (2.4) is also replaced by another rule that, although it also ensures the conservation of energy, will allow transitions "within" a given principal quantum number n. The resulting spectral lines arise from the **hyperfine structure** of the Hamiltonian. Any potential transition that does not obey these rules is said to be **strictly forbidden**.

Let us consider an example for the hydrogen atom where $n = 1$ and, therefore, $L = 0$. Because the electron and the proton have $S = I = 1/2$ and

$$F = 0 \text{ and } 1. \tag{2.10}$$

We thus find that within the so-called ground state of the atom there can be radiative transitions within it. The photons involved have the wavelength of the celebrated **21 cm line**. The corresponding energy is 5.9×10^{-5} eV.

But because this line is forbidden (but not strictly forbidden) the probability of a **spontaneous emission** of the type $F = 1 \rightarrow 0$ is very low. Accordingly, the lifetime of the $F = 1$ state is very long at approximately 10^7 yr. Even so, because of the large number of atoms populating some regions of the interstellar medium it is possible to detect large signals at that wavelength. Furthermore, since the excitation from $F = 0 \rightarrow 1$ within the state $n = 1$ in the cold interstellar medium are primarily due to collisions, the intensity of the detected spectral lines are proportional to the collision rate and, therefore, the density or, more precisely, the **column density** N_{HI} of atomic hydrogen. Using the 21 cm line radio astronomers have been able to map the surface density of atomic hydrogen within the Galaxy as a function of distance to the Galactic centre. The radial distance can be evaluated by matching the observed systemic velocity of the line with the well-known Galactic rotation model. The result is shown in Figure 2.1. The main features include:

- The HI gas pervades the Galactic disk between radii of 4 kpc and 8.5 kpc with a scale height of approximately 100 pc.
- In the outer Galaxy the scale height increases linearly with radius.
- At furthest radii the HI layer warps by several kpc from a perfect plane.
- The gas distribution is not uniform. The so-called **cold neutral medium (CNM)** has temperatures ranging from approximately 40 to 160 K. Most of this gas is concentrated in **HI clouds** with number densities and diameters ranging from 10 to 100 cm^{-3} and 1 to 100 pc, respectively. It contains a total mass of about $3 \times 10^9 M_\odot$.
- The scale height is regulated, in part, by the velocity dispersion (approximately 6 km/s) of the HI clouds.
- Whatever gas not contained in clouds is distributed widely at twice the scale height of the CNM, at a density of 0.5 cm^{-3} and a temperature of approximately 8,000 K. This is the so-called **warm neutral medium (WNM)**, containing a total mass of about $4 \times 10^9 M_\odot$.

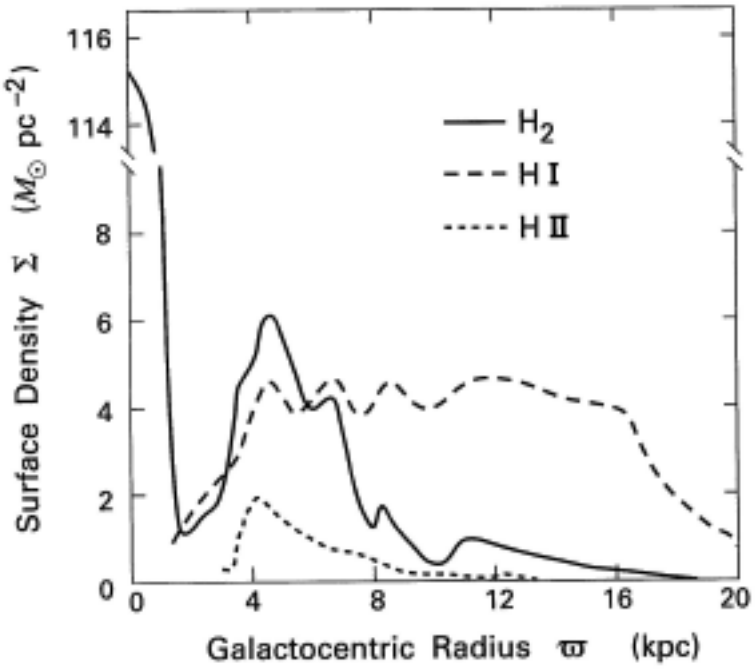

Figure 2.1 – Surface density of the H_2, HI, and HII as a function of Galactic radius. The HII map only includes the gas contained in HII regions.

2.1.2 **Ionized Hydrogen - HII Regions**

As we already know, O and B stars in OB associations will ionize the gas surrounding them. As electrons recombine with protons it can cascade down through the different energy levels of the bound hydrogen atom creating a huge number of observable spectral lines (e.g., the Lyman and Balmer series). Some of these lines are a result of transitions between two high energy levels that are very close (see equation (2.1)) and lie at radio wavelengths. It follows that ionized hydrogen (and HII regions) can be mapped in the same way as atomic hydrogen. The result of such study is also shown in Figure 2.1. It is found that:

- This ionized gas has a temperature of about 8,000K and its density peaks at 5 kpc from the Galactic centre.
- The total mass contained in HII regions is approximately $1\times10^8\,M_\odot$.

2.1.3 **Molecular Gas – H_2**

The temperature of the typical molecular cloud is so low (on the order of 10 K) that the molecular species that make up the gas can only be in their respective electronic and vibrational ground states (we will discuss molecular spectroscopy in a later chapter). This has for consequence that only **rotational transitions** can used to map the gas within the Galaxy. But the interaction of a molecule with an electromagnetic field happens mainly through its electric dipole moment (other interactions such as the electric quadrupole interaction generally produce much weaker lines that are very difficult to detect in most

parts of a molecular cloud). Unfortunately, molecular hydrogen in its ground electronic state is a symmetric molecule and has, therefore, no electric dipole moment. The sad consequence resulting from this fact is that the main component of the molecular gas (i.e., H_2, 70% by mass) is undetectable! Because of this other molecules, assumed coexistent with molecular hydrogen, must be used to map the contents of molecular clouds. Carbon monoxide (CO, and also its isotopologues (e.g., ^{13}CO and $C^{18}O$)) is a molecule of choice for this because of its relatively high abundance and the strength of its rotational lines. The results from CO mapping studies are shown in Figure 2.1. It is found that the Galactic distribution of H_2 is quite different from that of HI in that:

- There is a very strong concentration of H_2 at the Galactic centre with a very steep decline at a radius of approximately 1 kpc.
- There is a prominent **molecular ring** between radii of about 3 kpc to 8 kpc, and very little molecular gas beyond 10 kpc.
- The gas is concentrated in molecular clouds that are located in the vicinity of the Galactic plane, with a scale height of 60 pc. The velocity dispersion of the ensemble of clouds is approximately 4 km/s.
- The total mass contained in molecular clouds is about $2 \times 10^9 M_\odot$.

2.1.4 **Warm and Hot Intercloud Gas**

There are theoretical and observational evidence that point to the existence of a **hot intercloud (and ionized) medium** of temperature on the order of 10^6 K and 0.003 cm^{-3} density, as well as a **warm ionized medium** of similar density (0.3 cm^{-3}) and temperature (8,000 K) as the WNM filling the space available between the clouds.

A summary of the properties of the components of the interstellar medium is presented in Table 2.1.

2.1.5 **Pressure Equilibrium**

Examination of the properties of the different components populating the interstellar medium, except the molecular gas, reveals an interesting fact. If we calculate the quantity $nT = P/k_B$ (P is the pressure), we find values that all approach $4{,}000$ cm^{-3} K to better than a factor of two or three. This perhaps remarkable fact brings to front that the idea that the different phases of the interstellar medium are in pressure equilibrium.

The molecular gas must be left out of that model since large concentrations of gas imply that self-gravity cannot be neglected. More precisely, the requirement for some sort of mechanical equilibrium will bring pressures that are much larger than that of the other phases at the centre of the clouds. Although the pressure at the boundary of a molecular cloud must match that of the intercloud medium if it is not to contract or expand, the molecular gas is usually not considered as a distinct phase on the interstellar medium because of these high central pressures.

Table 2.1 – Phases of the Interstellar Medium - f is the volume-filling factor.

Phase	$n_{\rm tot}$ ($\rm cm^{-3}$)	T (K)	M ($10^9\,M_\odot$)	f
Molecular	>300	10	2.0	0.01
Cold neutral	50	80	3.0	0.04
Warm Neutral	0.5	8,000	4.0	0.3
Warm ionized	0.3	8,000	1.0	0.15
Hot ionized	0.003	500,000	—	0.5

2.2 Interstellar Dust

Dust grains, which stand of the way of radiation as it makes it to our telescopes, absorb light at short wavelengths (optical and ultraviolet → heating) and emit radiation at longer wavelengths (far infrared and submillimetre → cooling). These simple facts need to be carefully accounted for when either studying the detection of starlight or radiation from the dust grains themselves.

2.2.1 Extinction and Reddening

It is easy to show from equation (1.4) that the observed magnitude m_λ from a star of absolute magnitude M_λ at wavelength λ and at a distance r is given by

$$m_\lambda = M_\lambda + 5\log\left(\frac{r}{10\ \rm pc}\right) + A_\lambda, \tag{2.11}$$

where A_λ is the **extinction** at wavelength λ. This extinction is a positive quantity that accounts for the dimming of the star by the intervening interstellar dust. We also define the **intrinsic color index** at wavelengths λ_1 and λ_2 as

$$C^\circ_{12} \equiv M_{\lambda_1} - M_{\lambda_2}, \tag{2.12}$$

and likewise the **observed color index** at the same wavelengths

$$\begin{aligned} C_{12} &\equiv m_{\lambda_1} - m_{\lambda_2} \\ &= \left(M_{\lambda_1} - M_{\lambda_2}\right) + \left(A_{\lambda_1} - A_{\lambda_2}\right) \\ &= C^\circ_{12} + E_{12}, \end{aligned} \tag{2.13}$$

where

$$E_{12} \equiv \left(A_{\lambda_1} - A_{\lambda_2}\right) \tag{2.14}$$

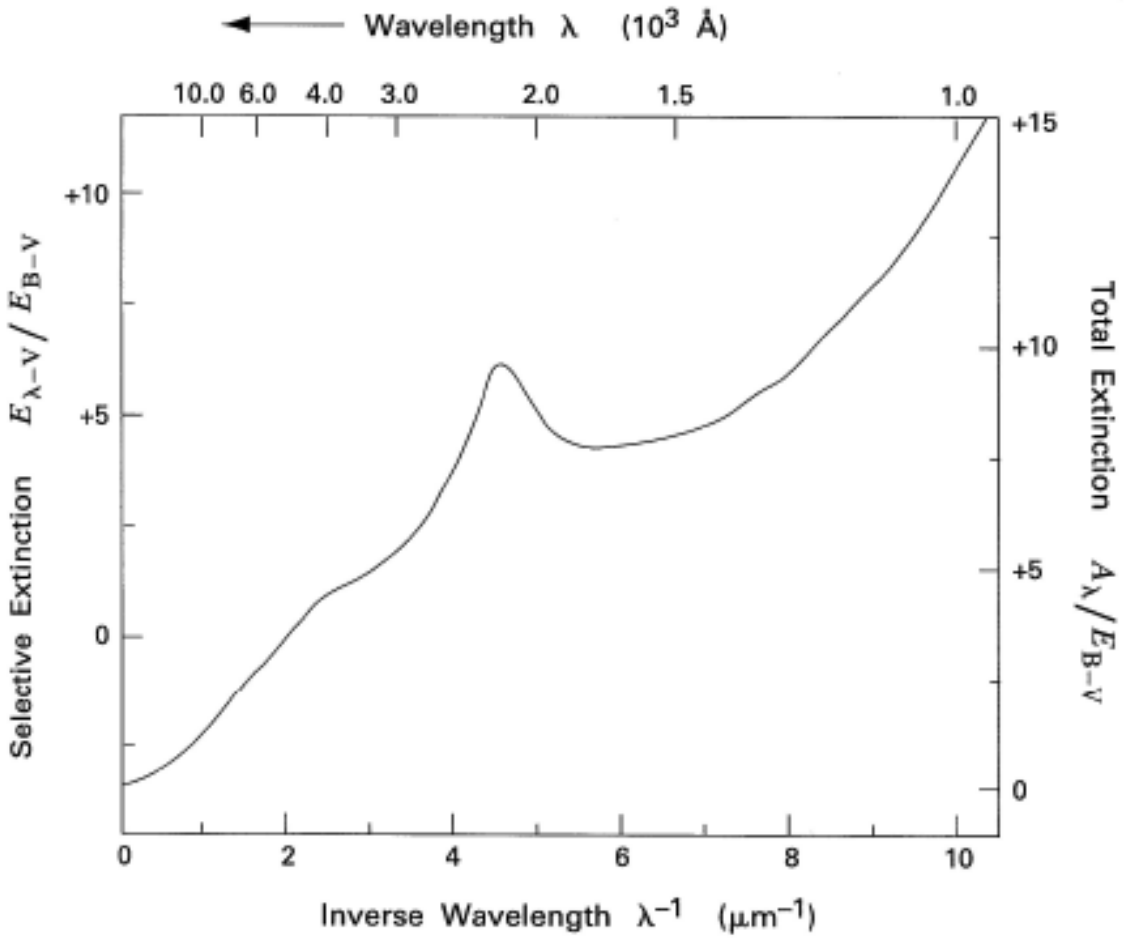

Figure 2.2 – The Interstellar extinction curve.

is the **color excess**. The color indices and the color excess are often written as $(U-B)_\circ$, $(U-B)$, and E_{U-B}, respectively, as a function of specific wavelengths, U and B in this case.

Now consider the so-called **selective extinction**

$$\begin{aligned}\frac{E_{\lambda-V}}{E_{B-V}} &= \frac{A_\lambda}{E_{B-V}} - \frac{A_V}{E_{B-V}} \\ &= \frac{A_\lambda}{E_{B-V}} - R,\end{aligned} \tag{2.15}$$

with the (normalized) **total extinction**

$$R \equiv \frac{A_V}{E_{B-V}} = 3.1. \tag{2.16}$$

The quoted value is an average and can fluctuate depending on the region studied. As can be hinted by the fact that the quantity R is averaged to a constant, the advantage gained in considering relations like those in equations (2.15) and (2.16) is that they don't depend on the amount of dust encountered by the detected radiation, unlike quantities such as the extinction and the intrinsic color index and the color excess. Evidently this is the kind of tools we need in order to characterize interstellar dust. An example of this is showed in Figure 2.1 where the interstellar extinction curve is plotted. The value of R quoted in equation (2.16) can be determined with this curve, as the first term on the right-hand side of equation (2.15) goes to zero in the long-wavelength limit.

2.2.2 **Basic Radiative Transfer**

We now consider the same problem but with a more analytical approach. We first define the **specific intensity** I_ν as the energy per unit time, per unit frequency, per unit area, and per unit solid angle (see Figure 2.3) at frequency ν.

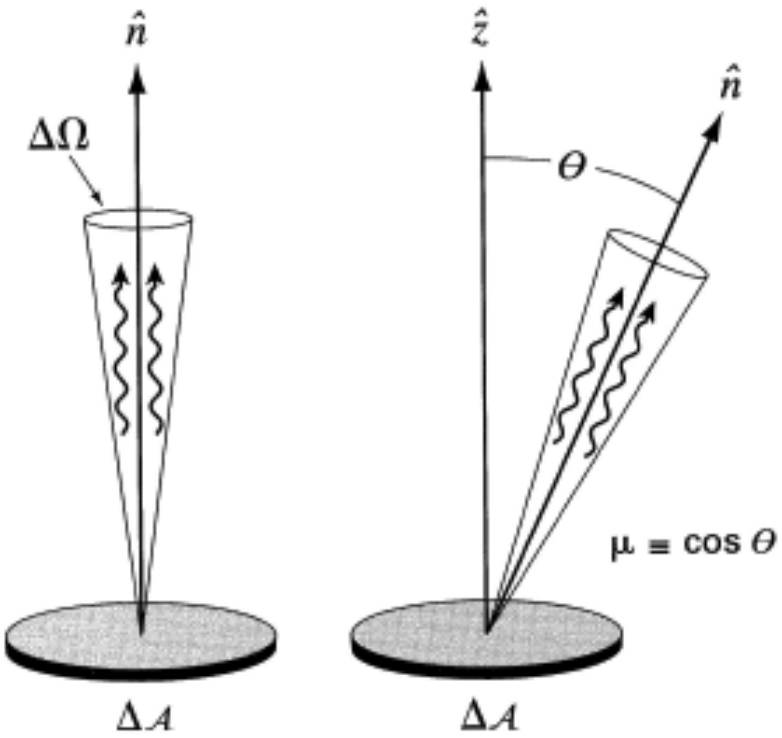

Figure 2.3 – Definition of the specific intensity; $\hat{n}$ and $\hat{z}$ are unit vectors.

Other important and useful quantities are the **specific flux**

$$F_\nu = \int I_\nu \, \mu \, d\Omega, \tag{2.17}$$

with $\mu = \hat{n} \cdot \hat{z}$ (see Figure 2.3), the **energy density**

$$u_\nu = \frac{1}{c} \int I_\nu \, d\Omega, \tag{2.18}$$

since radiation travels at the speed of light c, and the **mean intensity**

$$J_\nu = \frac{1}{4\pi} \int I_\nu \, d\Omega. \tag{2.19}$$

As radiation travels through the interstellar medium it can be scattered, absorbed, or enhanced with new, localized emission. If we denote the **opacity** by κ_ν, in $\mathrm{cm^2 g^{-1}}$, and the **emissivity** j_ν, in energy per unit time, volume, frequency, and solid angle, then the variation of the specific intensity as a function distance traveled is easily shown to be

$$\frac{dI_\nu}{ds} = -\rho \kappa_\nu I_\nu + j_\nu, \tag{2.20}$$

where ρ is the mass density of the material that causes the extinction. Equation (2.20) is the **equation of transfer**. The infinitesimal **optical depth** is defined (although sometimes with the opposite sign)

$$d\tau_\nu = \rho \kappa_\nu ds, \tag{2.21}$$

and $1/\rho\kappa_\nu$ the **photon mean free path**.

2.2.3 Extinction and Optical Depth

Using equation (2.21), equation (2.20) can be transformed as follows

$$\frac{dI_\nu}{d\tau_\nu} + I_\nu = S_\nu, \tag{2.22}$$

with S_ν the **source function**. If we assume that the source function within a homogeneous slab of material is constant and that the specific intensity "behind" it is denoted by $I_\nu(0)$, then we can easily solve this equation (using Laplace transforms; e.g., $I_\nu(s)$ is the Laplace transform of I_ν)

$$I_\nu(s)(s+1) - I_\nu(0) = \frac{S_\nu}{s}, \tag{2.23}$$

or

$$I_\nu(s) = \frac{S_\nu}{s(s+1)} + \frac{I_\nu(0)}{(s+1)}, \tag{2.24}$$

and

$$I_\nu = S_\nu\left(1 - e^{-\tau_\nu}\right) + I_\nu(0)e^{-\tau_\nu}. \tag{2.25}$$

If we assume that the slab (i.e., the interstellar medium) does not emit and set $S_\nu = 0$ and that $I_\nu(0)$ is for the radiation emanating from the photosphere of a star of radius R_*, then the specific flux measured at a distance r is given by

$$\begin{aligned} F_\nu(r) &= I_\nu(0)e^{-\tau_\nu}\int \mu\, d\Omega \\ &= \pi I_\nu(0)\left(\frac{R_*}{r}\right)^2 e^{-\tau_\nu}, \end{aligned} \tag{2.26}$$

since $\mu \simeq 1$, $d\mu \simeq \theta d\theta$, with $0 \le \theta \le R_*/r$. Evidently, if there were no material between the star and the observer, then the optical depth would be zero. If we further denote the flux measured in such conditions at a the distance of 10 pc by $F_\nu^*(10\text{ pc})$, then we can write

$$F_\nu(r) = F_\nu^*(10\text{ pc})\left(\frac{10\text{ pc}}{r}\right)^2 e^{-\tau_\nu}, \tag{2.27}$$

and

$$-2.5\log\left[F_\nu(r)\right] = -2.5\log\left[F_\nu^*(10\text{ pc})\right] + 5\log\left(\frac{r}{10\text{ pc}}\right) + 1.086\,\tau_\nu. \tag{2.28}$$

Comparison of equation (2.28) with equation (2.11) shows that the extinction is given by

$$A_\lambda = 1.086\,\tau_\lambda, \tag{2.29}$$

where we changed from frequency to wavelength space. Equation (2.29) renders clear the fact that extinction is caused by the scattering and absorbing material present in the intervening interstellar medium; dust grains in our case. We must remember that τ_λ is the total optical depth as the radiation travels from the source to the observer.

2.2.4 **Blackbody Radiation**

The stellar radiation absorbed by the dust grains will heat them up. It follows that if they are to attain some sort of thermal equilibrium, the same dust grains must radiate and cool off is such way as to cancel out the constant heating provided by the absorbed radiation. Because of their size (0.1 μm on average) the grains will absorb mainly at optical and ultraviolet wavelengths. The equilibrium temperature they eventually reach is function of many parameters (distance to radiation sources, their composition, etc.) and generally observed to be low in molecular clouds, on the order of 10 K.

To determine the range of wavelengths at which the dust will radiate most effectively, we approximate the grains as **blackbody radiators**. In this case the radiation is uniform and isotropic, and the specific intensity is given by famous **Planck function**

$$B_\nu(T) = \frac{2h\nu^3/c^2}{e^{h\nu/k_B T} - 1}, \tag{2.30}$$

or

$$B_\lambda(T) = \frac{2hc^2/\lambda^5}{e^{hc/\lambda k_B T} - 1}. \tag{2.31}$$

Equating the appropriate derivative in these two equations to zero, we can verify that the frequency and wavelength of maximum intensity are given by the **Wien displacement law**

$$\begin{aligned} \frac{\nu_{\max}}{T} &= 5.88 \times 10^{10} \text{ Hz K}^{-1} \\ \lambda_{\max} T &= 0.29 \text{ cm}. \end{aligned} \tag{2.32}$$

It is, therefore, easily verified that at 10 K the dust will radiate most efficiently at approximately 300 μm. The precise shape of different blackbody radiation spectra is shown in Figure 2.4.

If we further approximate the radiation spectrum of the star with the Planck function at its effective temperature T_{eff}

$$I_\nu(0) = B_\nu(T_{\text{eff}}), \tag{2.33}$$

then from equation (2.17)

$$F_\nu(0) = \pi B_\nu(T_{\text{eff}}). \tag{2.34}$$

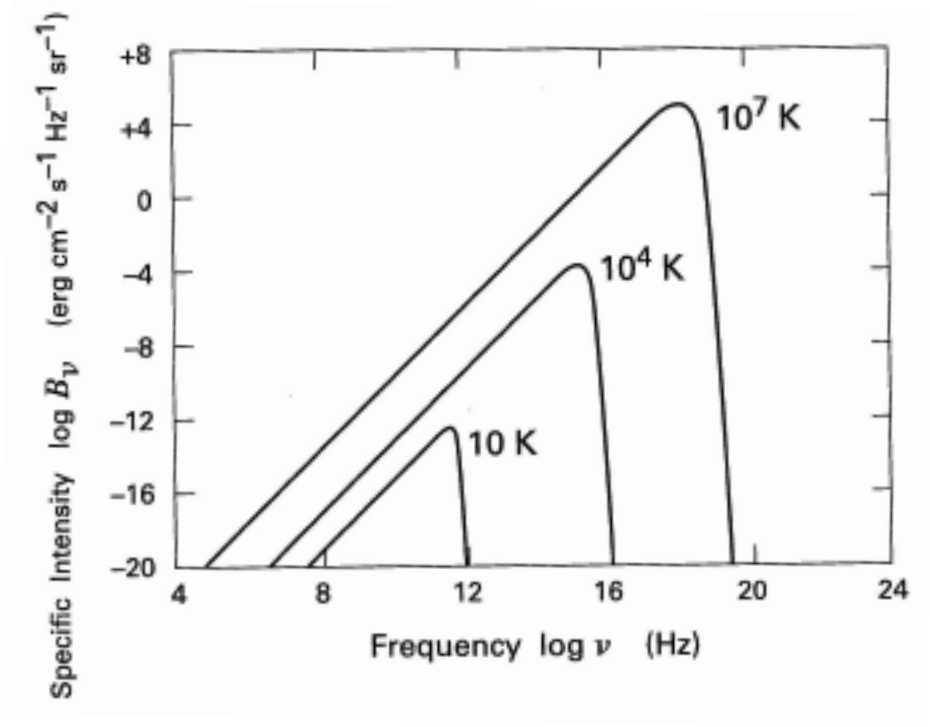

Figure 2.4 – Blackbody radiation spectra for different temperature as a function of frequency (note that 10^{12} Hz corresponds to 300 μm).

The bolometric flux is obtained through integration over frequency with

$$F_{\rm bol} = \sigma_{\rm B} T_{\rm eff}^2, \tag{2.35}$$

with the Stefan-Boltzmann defined as

$$\begin{aligned} \sigma_{\rm B} &\equiv \frac{2\pi^5 k_{\rm B}^4}{15 c^2 h^3} \\ &= 5.67 \times 10^{-5} \text{e erg cm}^{-2}\ \text{s}^{-1}\ \text{K}^{-4}. \end{aligned} \tag{2.36}$$

Accordingly the total bolometric luminosity (i.e., energy radiate per unit time, or the power) is given by (see equation (1.1))

$$L_* = 4\pi R_*^2 \sigma_{\rm B} T_{\rm eff}^2. \tag{2.37}$$

2.3 Properties of Interstellar Dust Grains

It should be clear that since the opacity κ_λ, of units $\mathrm{cm^2 g^{-1}}$, is the total area per unit mass causing the extinction, then the quantity $\rho\kappa_\lambda$ is the total extinction cross-section per unit volume. We can, therefore, write

$$\rho\kappa_\lambda = n_\mathrm{d}\sigma_\mathrm{d}Q_\lambda, \tag{2.38}$$

where n_d is the number density of dust grains, $\sigma_\mathrm{d} = \pi a_\mathrm{d}^2$ their mean physical cross-section (a_d is the mean radius), and Q_v is the **extinction efficiency factor**. We now consider the following ratio

$$\frac{Q_\lambda}{Q_0} = \frac{A_\lambda / E_{B-V}}{A_0 / E_{B-V}}, \tag{2.39}$$

where Q_0 and A_0 are evaluated in the high-frequency limit. In that extreme case, we would expect that the scattering and absorption cross-sections both equal the physical cross section. Since equation (2.38) stands for the extinction, which includes both processes, we surmise that $Q_0 = 2$. Moreover, inspection of the interstellar extinction curve of Figure 2.2 reveals that

$$\frac{A_0}{E_{B-V}} \approx 14. \tag{2.40}$$

We, therefore, find that

$$Q_\lambda = 0.14\frac{A_\lambda}{E_{B-V}}. \tag{2.41}$$

Using this relation and referring once again to the interstellar extinction curve we deduce by inspection that at optical wavelengths

$$Q_\lambda \propto \lambda^{-1}. \tag{2.42}$$

At longer wavelengths at which dust radiates, it is conventional to assume that

$$Q_\lambda \propto \lambda^{-\beta}, \tag{2.43}$$

with $1 < \beta < 2$.

Another useful quantity is the **total geometric cross-section per hydrogen atom**

$$\begin{aligned}\Sigma_{\rm d} &\equiv \frac{n_{\rm d}\sigma_{\rm d}}{n_{\rm H}} \\ &= \frac{N_{\rm d}\sigma_{\rm d}}{N_{\rm H}},\end{aligned} \tag{2.44}$$

where $N_{\rm d} = n_{\rm d}L$ and $N_{\rm H} = n_{\rm H}L$ stand for the corresponding **column densities** (L is for the linear size of the region concerned). Using equations (2.21), (2.29), and (2.41) we transform the first of equations (2.44) to

$$\begin{aligned}\Sigma_{\rm d} &= \frac{\tau_\lambda}{n_{\rm H}LQ_\lambda} \\ &= \frac{A_\lambda/1.086}{N_{\rm H}\left(0.14\,A_\lambda/E_{B-V}\right)} \\ &= 6.6\left(\frac{E_{B-V}}{N_{\rm H}}\right)\ {\rm cm}^2.\end{aligned} \tag{2.45}$$

The ratio of the color excess to the column density of hydrogen was measured observationally to be

$$\frac{E_{B-V}}{N_{\rm H}} = 1.7\times10^{-22}\ {\rm mag\ cm}^2. \tag{2.46}$$

It then becomes possible to determine the relationship between the column density of hydrogen and the visual extinction using equations (2.16) and (2.46), we get

$$\frac{N_{\rm H}}{A_V} = 1.9\times10^{21}\ {\rm mag}^{-1}\ {\rm cm}^{-2}, \tag{2.47}$$

and

$$\Sigma_{\rm d} = 1.1\times10^{-21}\ {\rm cm}^2. \tag{2.48}$$

Interestingly, we can also use equations (2.41) and (2.46) to find

$$\frac{N_{\rm H}}{A_V} = 7.9\times10^{20}Q_V\ {\rm mag}^{-1}\ {\rm cm}^{-2}, \tag{2.49}$$

which from equation (2.47) implies that

$$Q_V \simeq 2.4. \tag{2.50}$$

Finally, we use these relations to evaluate $f_{\rm d}$ the ratio of dust mass to gas mass present in the interstellar medium

$$\begin{aligned} f_{\rm d} &\equiv \frac{n_{\rm d} m_{\rm d}}{\mu n_{\rm H} m_{\rm H}} \\ &= \left(n_{\rm d} \rho_{\rm d} \frac{4\pi}{3} a_{\rm d}^3 \right) \Big/ \left(\mu n_{\rm H} m_{\rm H} \right) \\ &= \left(\frac{n_{\rm d} \pi a_{\rm d}^2}{n_{\rm H}} \right) \left(\frac{4 \rho_{\rm d} a_{\rm d}}{3 \mu m_{\rm H}} \right) \\ &= 1.84 \times 10^{19} \Sigma_{\rm d} \\ &= 0.02, \end{aligned} \tag{2.51}$$

where we used equations (2.44) and (2.48), $\rho_{\rm d} = 3$ g cm^{-3} for the average mass density of a dust grain, $a_{\rm d} = 0.1\ \mu$m for its average radius, and $\mu = 1.3$ for the average mass number of a gas particle relative to that of the hydrogen atom.